PAPER

Check for updates

Statistical assessment of an atmospheric mercury passive sampler at a regional site in South Africa†

Xoliswa E. V. Job,[a] Kerneels Jaars, [ID] *[a] Pieter G. van Zyl, [ID] [a] Katrina MacSween,[b] Liezl Bredenkamp,[a] Miroslav Josipovic,[a] Lynwill G. Martin,[ac] Ville Vakkari,[ad] Markku Kulmala [ID] [e] and Lauri Laakso[ad]

South Africa has been ranked among the top ten mercury (Hg) emitters globally, with emissions from coal-fired power plants being the most significant contributor. The expansion of atmospheric Hg measurement networks in southern Africa is vital within the global context but is constrained by high costs and logistics. Passive air samplers were developed to address these issues and expand atmospheric monitoring networks. A commercially available passive sampler widely used for atmospheric Hg monitoring is the Mercury Passive Air Sampler (*Mer*PAS®). Therefore, this study aimed to statistically evaluate the performance of these samplers in the unique South African environment by comparing Hg concentrations determined with *Mer*PAS® with active *in situ* atmospheric Hg measurements conducted in this region. Measurements were conducted from June 2021 to September 2022 at the Welgegund atmospheric monitoring station, considered one of Africa's most comprehensively equipped atmospheric measurement sites. Hg concentrations measured with *Mer*PAS® were derived for different sampling rates (SR), *i.e.* the original SR (OSR) provided by the supplier and an adjusted original SR (AOSR) derived using the OSR with adjustments for mean temperature and wind speed. Statistical analyses, including Kruskal–Wallis, Mann–Whitney U, Bland–Altman, and Spearman correlation tests, were used to assess the performance of *Mer*PAS®. The OSR overestimated Hg concentrations by 16%, while the AOSR reduced this overestimation to 10%, improving alignment with active sampling data. The Mean Normalized Difference (MND) also decreased from 17.4% with OSR to 12.7% with AOSR, indicating greater accuracy. Spearman correlation analysis showed moderate agreement between passive and active sampling, with correlation coefficients of 0.39 for OSR and 0.58 for AOSR, supporting the improved comparability of AOSR. Seasonal patterns were consistent across both methods, with elevated Hg levels observed in winter due to atmospheric inversions and increased emissions. Despite a slight positive bias, the Bland–Altman analysis further confirmed good reliability between the AOSR and active measurements. This study demonstrates that *Mer*PAS®, when calibrated for local environmental conditions, provides an accurate, cost-effective alternative for Hg monitoring, offering a feasible solution for expanding networks in regions with limited resources. By enabling broader and more accessible atmospheric Hg data collection, *Mer*PAS® can support critical environmental policies, such as the Minamata Convention, and deepen scientific understanding of Hg dynamics in under-monitored areas like southern Africa. These findings lay the groundwork for enhancing global Hg monitoring, contributing essential insights into regional pollution and atmospheric processes across diverse environments.

Environmental significance

South Africa is a top global emitter of mercury (Hg), primarily from coal-fired power plants. Expanding atmospheric Hg monitoring networks in southern Africa is critical but is hindered by high costs and logistical challenges. This study statistically evaluated the performance of a commercially available passive air sampler, the Mercury Passive Air Sampler (*Mer*PAS®), by comparing its Hg concentrations to active *in situ* atmospheric Hg measurements at a regional background site in South Africa from June 2021 to September 2022. Statistical analyses revealed that while *Mer*PAS® slightly overestimated Hg concentrations, adjustments for environmental factors improved its accuracy and alignment with active measurements. These findings highlight *Mer*PAS® as a cost-effective solution to expand Hg monitoring networks in resource-limited regions, supporting global and regional efforts to mitigate Hg pollution under the Minamata Convention.

[a]*Atmospheric Chemistry Research Group, Chemical Resource Beneficiation, North-West University, Potchefstroom, South Africa. E-mail: kerneels.jaars@nwu.ac.za*

[b]*Air Quality Research Division, Science and Technology Branch, Environment and Climate Change Canada, Toronto, Canada*

[c]*South African Weather Service c/o CSIR, Stellenbosch, South Africa*

[d]*Finnish Meteorological Institute, Helsinki, Finland*

[e]*Institute for Atmospheric and Earth System Research, University of Helsinki, Helsinki, 00014, Finland*

† Electronic supplementary information (ESI) available. See DOI: https://doi.org/10.1039/d4ea00071d

© 2025 The Author(s). Published by the Royal Society of Chemistry

Environ. Sci.: Atmos., 2025, **5**, 191–203 | 191

1 Introduction

In the last 20 years, South Africa has been ranked among the top ten mercury (Hg) emitters globally,[1] with emissions from coal-fired power plants being the most significant contributor.[2] These elevated Hg emissions raise substantial concerns due to their adverse effects on human health, particularly for pregnant women and the environment. Hg is a potent neurotoxin that accumulates in aquatic ecosystems, impacting fish and seafood, while airborne emissions contribute to global atmospheric pollution, emphasizing the urgent need for mitigation measures. According to Zhao et al.,[3] the Hg content in coal from South Africa (0.2 mg kg^{-1}) is higher than the world average (0.1 mg kg^{-1}). South Africa became a signatory of the Minamata Convention on Mercury in 2013, a global treaty aimed at reducing worldwide Hg emissions.[4] Since then, Hg has been identified as a pollutant of national future concern in South Africa.[5]

Given that the atmosphere represents the primary pathway for the global distribution of Hg,[6–8] monitoring atmospheric Hg is essential in achieving the above-mentioned objectives. Existing atmospheric Hg monitoring networks, such as the Global Mercury Observation System (GMOS), the Atmospheric Monitoring Network (AMNet), and the Environment and Climate Change Canada Atmospheric Mercury Monitoring Network (ECCC-AMM), have greatly improved our understanding of atmospheric Hg,[9] while it also contributed to the development of global atmospheric dispersion models[10] such as GEOS-Chem, GLEMOS, GEM-MACH-Hg and ECHMERITRADM.[11] However, the spatial coverage of these networks is limited, especially for the southern hemisphere and Africa,[9] which leads to large gaps in understanding atmospheric Hg cycling. Therefore, it is globally acknowledged that further network expansion is pivotal.[12,13]

The Global Atmospheric Watch (GAW) station at Cape Point (CPT), South Africa, represents the longest-running site for Hg monitoring in the southern hemisphere.[14–19] These studies highlighted complex transport and deposition dynamics, with biomass burning and shipping routes identified as significant contributors to atmospheric Hg. Bieser et al.[20] also emphasized the role of oceanic sources in the southern hemisphere Hg budget, suggesting that air–sea exchange may compensate for reductions in atmospheric emissions from the Minamata Convention.

While the above mentioned site provides a valuable long-term coastal baseline, its location limits insights into Hg levels in South Africa's industrialized inland regions. Despite the region's notable industrial activities and high air pollution levels, research on Hg levels in South Africa's interior remains limited. Recent short-term studies in the Highveld Priority Area[21,22] have provided initial Hg concentration data, yet comprehensive, long-term monitoring efforts in the region are lacking. Recognizing this gap, the South African Mercury Network (SAMNet) has been established to create a broader monitoring network, targeting both industrial and background locations. This initiative aims to yield spatially representative Hg data, offering a more comprehensive perspective on regional Hg dynamics.

However, the expansion of SAMNet is constrained by high costs, logistics (e.g. availability of electricity and specialized materials), as well as underdeveloped capacity and expertise (e.g. technical training). Addressing this deficiency in atmospheric Hg network coverage in South Africa is crucial to our global understanding of atmospheric Hg distribution and assessment of its impacts. In order to overcome these limitations in spatial coverage of atmospheric Hg monitoring, an alternative approach has been followed through the development of passive air samplers (PAS), which has the potential to significantly improve the spatial resolution of atmospheric Hg measurements.[12,23,24] These passive samplers offer a range of benefits, which include lower costs and no electricity requirements and can be deployed in large numbers, especially throughout South Africa. However, PAS does have certain limitations. One deficiency is the relatively longer collection time required to accumulate sufficient analyte, which limits the temporal resolution of the data obtained. Additionally, measurement of other than gaseous elemental mercury (GEM), such as gaseous oxidized mercury (GOM) and particulate-bound mercury (PBM) with PAS, remains challenging.

In passive sampling, the gaseous analyte diffuses through a barrier into a chamber at a known rate into the specially designed sampler. The analyte is trapped inside the chamber on a sorbent material, which is analyzed after deployment. One commercially available PAS widely used in Hg monitoring is the Mercury Passive Air Sampler (MerPAS®), developed by the University of Toronto and later commercialized by Tekran®. While MerPAS® relies on diffusion, other PAS designs, such as the two-bowl PUF-PAS, rely on a flow-through approach using airflow.[25] This sampler has a unique design that utilizes sulphur-impregnated activated carbon as the sorbent material and incorporates a diffusive barrier to control the sampling rate. It also features a protective shield, allowing deployment in outdoor environments for extended periods. The MerPAS® method has been evaluated globally at atmospheric monitoring sites in different environments with variable atmospheric Hg concentrations.[26,27] Recently, Naccarato et al.[26] showed that MerPAS® is currently the best available passive sampler for GEM concentration monitoring, while McLagan et al.[28] indicated that the precision of these samplers is 3.6 ± 3.0%, with an overall uncertainty of 8.7 ± 5.7% when compared to active measurements of several PAS globally deployed. However, the performance of these samplers has not been evaluated within South Africa in any of these studies.

Therefore, this study aims to evaluate the accuracy, precision and reliability of MerPAS® statistically, specifically in the unique South African environment, by comparing Hg concentrations determined with these samplers with well-established active in situ atmospheric Hg measurements conducted in this region. MerPAS® was deployed at a comprehensively equipped regional atmospheric monitoring station in the South African interior, which provides a reliable benchmark for comparison. Measurements were conducted through the recently established South African Mercury Network (SAMNet), which aims to expand the spatial resolution of atmospheric Hg measurements conducted in this region. The use of MerPAS® is crucial to the successful rollout and establishment of this expanded atmospheric Hg monitoring network.

2 Methods

2.1 Site description

Measurements were conducted at the Welgegund atmospheric measurement station (26.57°S, 26.94°E, 1480 m above sea level) from June 2021 to September 2022. A detailed description of the site in terms of geographical location, meteorology and vegetation type is presented in numerous papers.[29–36] The site is located on a commercial farm approximately 100 km southwest of Johannesburg, as indicated in Fig. 1. Although no large point sources are near Welgegund, the site is impacted by the major source regions in the north-eastern South African interior, as indicated in Fig. 1. In addition, air masses passing over a relatively clean western sector also impact Welgegund (Fig. 1). Previous research has demonstrated the influence of these regional sources on the atmospheric composition at Welgegund. During the sampling period in this study, meteorological conditions were characterized by an average temperature of 15.5 ± 6.5 °C (ranging between −6.9 and 37.7 °C) and an average relative humidity of 51.4 ± 24.5% (ranging between 4.7 and 100%). The total rainfall during the study period was 1021.5 mm. The prevailing wind direction was from the north-northwest, with an average speed of 3.6 ± 2.9 m s^{-1} (ranging between 0 and 6.9 m s^{-1}).

2.2 Measurements

2.2.1 *MerPAS®*. The theory and functioning of *MerPAS®* have been described in detail in the literature.[27,28,37–40] This sampler incorporates a cylindrical stainless-steel mesh containing sulphur-impregnated activated carbon (HGR-AC; Calgon Carbon Corporation) as the sorbent material. The mesh is placed within a microporous diffusive barrier (white Radiello®, Sigma-

Aldrich), which regulates the sampling rate. GEM diffuses through the barrier and is retained by the sorbent. The diffusive barrier is securely attached to a protective shield designed for outdoor deployment, featuring an opening at the bottom to facilitate air circulation and prevent exposure to precipitation. The rate at which *MerPAS®* absorbs GEM is minimally influenced by meteorological factors, *e.g.* wind speed and temperature.[38]

MerPAS® utilized in this study were prepared and shipped directly from the manufacturer (Tekran® Instruments cooperation). The samplers were sealed tightly with vinyl electrical tape, individually placed into zip-lock plastic bags, and shipped and stored in sturdy foam-lined aluminium or hard plastic cases. At Welgegund, three *MerPAS®* were removed from the plastic bags. The solid lids of two samplers were removed and replaced with black mesh screens, with their top facing into the samplers. The third *MerPAS®* was used as a blank to monitor contamination during the sampler assembly, handling, transport, and storage. A field blank was used for every deployment and was exposed for about four weeks, with the last blank exposed for almost 14 weeks. This was done to evaluate if the field blank contamination increased with deployment duration, and it was found that blank levels were much lower in the longer exposure time. Duplicate *MerPAS®* were deployed monthly from June 2021 to September 2022. These samplers were attached to a mounting bracket 4 m above ground level, with the open side of the samplers facing downward. After exposure, *MerPAS®* was removed from the mounting brackets, capped, sealed with polytetrafluoroethylene tape, again placed in plastic bags, and shipped in the aforementioned plastic cases to the Environment and Climate Change, Canada for analysis.

The *MerPAS®* were analyzed with a Direct Mercury Analyzer (DMA-80; Milestone Inc., Shelton, CT, USA), which determines the total Hg mass absorbed by the passive sampler by thermal
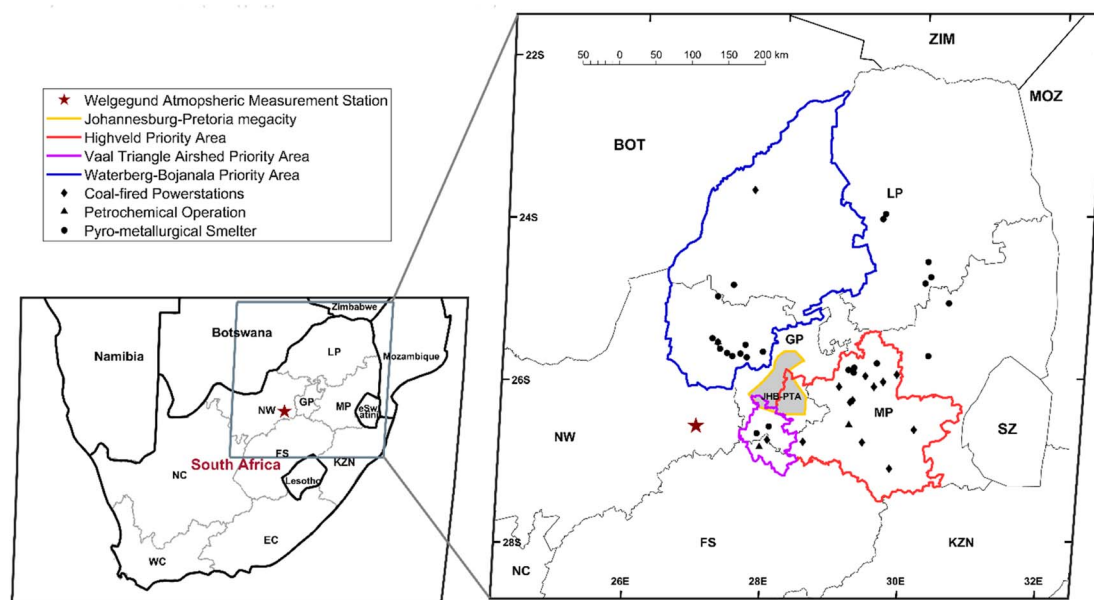

Fig. 1 Map of southern Africa with the zoomed-in area presenting the Welgegund atmospheric monitoring station (red star) in relation to major large point sources impacting air masses measured at Welgegund. Also indicated are the Jhb-Pta megacity and the three air quality priority areas as identified by the South African government.

© 2025 The Author(s). Published by the Royal Society of Chemistry

Environ. Sci.: Atmos., 2025, **5**, 191–203 | **193**

desorption and amalgamation. The analysis followed the modified US EPA method 7473, which is commonly used to determine Hg in complex matrices such as fish, sediment, and coal.[41–43] Prior to analysis, the stainless-steel cartridges of the MerPAS® containing the carbon sorbent were removed and separated into two sample aliquots. The two samples are then summed preceding analysis to determine the total Hg collected by the MerPAS®. Individual samples aliquots are coated in ~0.5 g of Sodium Carbonate (Na$_2$CO$_3$). Approximately 5 g Na$_2$CO$_3$ is also used to modify the catalyst tube. The Na$_2$CO$_3$ is used to limit the impact of the high sulphur content of the carbon sorbent that can cause poisoning of the catalyst and minimize analytical artefacts.[44] The samples were then thermally decomposed at 570 °C within the catalyst tube, releasing Hg from the carbon sorbent. Oxygen is then used to pull the released Hg through the catalyst and trapping all realized Hg on the gold amalgamator. The amalgamator is then heated to 900 °C to release Hg, which is then subsequently quantified by atomic absorption spectroscopy at a wavelength of 253.7 nm. Instrument recovery was tested every 15 to 20 samplers using 10 ng liquid Hg standards, and precision was tested every 30 samples using standard reference material, SRM NIST 2685c bituminous carbon 5% sulfur (NIST reported concentration 149.4 ± 4.5 ng g^{-1}). The average SRM NIST 2685C concentration was 146.8 ng g^{-1} (SD 11.11, $n = 7$) and a recovery of 98.3%. 10 ng Hg liquid standard averages 10.31 ng (SD 0.73, $n = 13$), with an average recovery of 103.1%. The DMA undergoes a full calibration if the recovery tests drift beyond 5% every time the catalyst is replaced. Calibration curves are established using liquid Hg standards of increasing concentrations on clean HGR-AC.

2.2.2 Active sampling. Continuous *in situ* atmospheric GEM measurements were conducted during the sampling period when MerPAS® was deployed with a Tekran® 2537X ambient Hg cold vapour atomic fluorescence spectrometer (CVAFS) equipped with a mass-flow controller (MFC) to ensure precise control of gas flow. The MFC is crucial for accurate measurements of GEM at high-altitude environments such as Welgegund. The Tekran® 2537X has a 5 minutes sampling frequency, and these values were averaged to the same period that MerPAS® was deployed. GEM concentrations were determined by alternating collection and analysis of one of the two gold traps within the analyzer. The analysis phase is initiated by heating a gold trap to ~500 °C, releasing the sorbed Hg into pure argon gas (>99.999% purity, Afrox), which carries the Hg to the detector. The analyzer was automatically calibrated every 24 hours using an internal permeation source. Site visits were conducted weekly to ensure the instrument was fully operational according to a predetermined checklist.

Data coverage over the 14 months sampling period was high, with the Tekran® 2537X capturing GEM measurements consistently. Weekly site visits, automated 24 hours calibrations, and an MFC minimized data interruptions, ensuring the reliability of the active dataset. Fig. S1† provides a visual summary of the percentage of data successfully captured, offering transparency in data continuity and supporting the comparability between active and passive sampling methods.

2.3 Data quality and calculations

Hg concentrations measured with MerPAS® were calculated from the blank-corrected Hg mass according to eqn (1):[45]

$$C = \frac{m}{(\text{SR} \times t)}, \tag{1}$$

where C (ng m^{-3}) is the Hg concentration, m (ng) is the blank-corrected Hg mass, t deployment time (days), and SR (m^3 per day) is the sampling rate of the MerPAS®. Similar to McLagan *et al.*,[28] two sets of atmospheric Hg concentrations were derived from the measured m in this study. The first concentration was derived by using the SR provided by Tekran for the MerPAS® (0.111 ± 0.017 m^3 per day), which we termed the original SR (OSR). The second concentration was derived using the OSR with adjustments for mean temperature (T_{exp}, °C) and wind speed (WS$_{\text{exp}}$, m s^{-1}) (hence the term adjusted original SR (AOSR)), recorded during the deployments in this study. The adjusted SR was calculated according to eqn (2), which was then used in eqn (1) to derive the concentration:

$$\text{SR}_{\text{adj}} = \text{SR} + \left(T_{\text{exp}} - 9.89\,°\text{C}\right) \times 0.0009\,\frac{\text{m}^3}{\text{day}\,°\text{C}}$$
$$+ \left(\text{WS}_{\text{exp}} - 3.41\,\frac{\text{m}}{\text{s}}\right) \times 0.003\,\frac{\text{m}^2\,\text{s}}{\text{day}}; \tag{2}$$

Table S1† summarises all these parameters utilized in calculating Hg concentrations with MerPAS®. On average, blank contamination in the MerPAS® deployed at Welgegund was 10% (ranging between 7% and 14%, Table S1†) of the amount quantified in an exposed sampler, which is in the same range as determined in other studies.[26,46]

2.4 Data filtering, statistical analysis and descriptive statistics

Statistical analysis and visualization were done using IBM SPSS Statistics version 29 for Windows, fit-for-purpose scripts in Matlab R2023b and R Statistical language (version 4.2.2;[47]) on Windows 10 × 64 (build 22 621). The specific R packages used that were central to this study were ggplot2 (version 3.5.0;[48]), tidyverse (version 2.0.0;[49]), ggpubr (version 0.6.0;[50]), ggpmisc (version 0.5.2;[51]) rstatix (version 0.7.2;[50]), and ggStatsplot (version 0.12.2;[52]). The seed was set to 123.

We first checked the concentrations obtained with the active *in situ* measurement and those derived from MerPAS® with the OSR and AOSR for outliers using the identify outliers function of the rstatix package. Outliers were identified but were not extreme. As a result, these outliers were kept in the data since they were detected for measurements taken in July, which is the middle of winter when Hg concentrations are usually high for the South African interior.[21,30,32,33]

To test for differences between concentrations derived from the active *in situ* measurement and those derived from MerPAS® using four SRs, a one-way ANOVA was conducted using IBM SPSS version 29 for Windows. Standardized residuals were saved so that the compliance with the requirements for ANOVA (normally distributed residuals, homogeneity of variance) could

be tested using the Kolmogorov–Smirnov one-sample and Levene's test. These tests revealed that the requirements of equal variance were met, but not normality, even when the dataset was $\log_{10}(x)$ transformed. Therefore, non-parametric tests were performed since only one requirement was met. The Mann–Whitney U test was used to compare two methods, and the Kruskal–Wallis test was used to compare more than two. At the same time, we used epsilon squared (ε^2) to assess the effect size.

Spearman's correlation coefficient (ρ(rho)) was employed to assess the linear relationship between concentrations obtained from the active *in situ* measurement and those derived from *Mer*PAS® using the OSR and AOSR. The general guidelines we used for interpreting the *p*-value, ρ, *r* and ε^2 are provided in ESI Table S2.†[53] In addition, exploratory, descriptive statistic calculations (mean, median, minimum, maximum, and standard deviation) were performed on the dataset to gain a general overview of variations in monthly average concentrations. For all statistical significance tests, we assume the null hypothesis to indicate a similar distribution while the alternate hypothesis suggests that statistically significant differences exist in the compared distributions. We use the significance level, *i.e.* alpha as 0.05, to accept or reject the null hypothesis.

Furthermore, we use the Bland–Altman analysis to identify any systematic biases or trends between the active *in situ* and any specific *Mer*PAS® with the OSR and AOSR and determine the magnitude and direction of the differences between the methods. This statistical analysis provides valuable insights concerning measurement methods' accuracy, precision, and agreement. We used the *eirasagree* package in R, developed by Silveira *et al.*,[54] to create a Bland–Altman plot and analyze our data to determine the agreement between concentrations from the active *in situ* measurement and those derived from *Mer*PAS® using four SRs.

The mean normalized difference (MND) and relative standard deviation (RSD) were also calculated for the datasets obtained from *Mer*PAS® with the four SRs in relation to the active *in situ* measurements. MND and RSD also reflect the accuracy and variability in datasets. The MND is calculated as follows:

$$\text{MND\%} = \left(\frac{1}{n} \sum_{i=1,n} \frac{|C_{\text{ACT},i} - C_{\text{PAS},i}|}{C_{\text{ACT},i}} \right) \times 100, \qquad (3)$$

where *n* is the number of comparisons, C_{PAS} (ng m^{-3}) is the *Mer*PAS® derived Hg concentrations and C_{ACT} (ng m^{-3}) monthly average Hg levels are determined with the active *in situ* measurements. RSD is calculated by dividing the standard deviation of a dataset by its mean and then multiplying it by 100. Lower MND values indicate good agreement between datasets, whereas lower RSD implies all data points are relatively close to the mean of the dataset.

3 Results and discussion

3.1 Blan concentrations

Field blanks are crucial for reliable sampling with *Mer*PAS® since they directly impact the method detection limit (MDL) and practical quantification limit (PQL). During the *Mer*PAS® sampling period at Welgegund, nine field blanks were utilized.

These field blanks contained mercury (Hg) content ranging from 0.381 to 2.417 ng g^{-1}, with an average concentration of 1.107 ± 0.817 ng g^{-1}. Considering the transportation and storage conditions of the *Mer*PAS® deployed at Welgegund, this study's average concentration of field blanks can be regarded as relatively low and comparable to findings from other studies. The Hg concentrations in the field blanks were used to calculate the MDL (three times the standard deviation) and PQL (ten times the standard deviation), which were determined to be 0.17 ± 0.14 ng and 0.58 ± 0.45 ng, respectively. Notably, none of the exposed passive samplers in our study exceeded the MDL and PQL.

To put these findings into context, Fig. S2† compares the mean blank concentration for Hg in this study with those reported in other studies utilizing passive sampling for mercury. It is worth noting that achieving blank levels below or around 0.5 ng g^{-1} is only possible when there is minimal transportation and limited storage time after sampling.[26,27,37,38,46] Studies involving transportation over regional distances, extended sampler storage, and sampling at Hg-contaminated sites have indicated slightly higher blank levels ranging from 0.5 ng g^{-1} to 2 ng g^{-1}.[39,55]

However, there have been instances where field blank levels have exceeded 3 ng g^{-1}. Examples include a study involving 20 global sampling sites,[28] measurements conducted at a gold mine in Ghana,[56] and a site in New Zealand.[57] Moreover, studies conducted in extreme and remote environments, such as the Antarctic plateau, Amsterdam Island, and La Réunion, have also reported blank levels higher than 3 ng g^{-1}.[46]

3.2 Replicate precision of the *Mer*PAS®

The precision-based uncertainty (RSD%) of the *Mer*PAS® sampler, as calculated from the successful replications in this study, was found to be 14 ± 13%. This is considerably higher than previously reported in the literature. For comparison, McLagan *et al.*[45] reported an RSD% between triplicate samplers of 4 ± 2% and 2 ± 1% for indoor and outdoor experiments, respectively. McLagan *et al.*[27] reported a 2 ± 2% value in their studies conducted in Toronto and Italy. Whereas McLagan *et al.*,[28] in their global calibration and evaluation study involving 129 replicated deployments, yielded a mean RSD of 3.6 ± 3.0%. Naccarato *et al.*[26] observed a replicate precision of 3%, which increased with deployment length from approximately 5% for two-weeks samples to around 2% for 12 weeks samples.

Other researchers have reported varying levels of precision. Quant *et al.*[55] reported a precision of 7.5%, Skov *et al.*[58] reported 7.7%, Zhang *et al.*[59] reported 10%, Hoang *et al.*[46] reported a range of 8–39%, and Snow *et al.*[56] reported a range of 1.1–17.5% and 0.9–5.7% for low and high concentration conditions, respectively. Cho *et al.*[60] observed replicate precision of GEM concentrations in different groups over different deployment times, ranging from 8.2% to 1.8%.

The relatively poor replicate precision observed in the present study can be attributed to various factors. These include the blank correction, which represents a relatively large fraction of the sequestered amount of Hg, as well as the relatively high

© 2025 The Author(s). Published by the Royal Society of Chemistry

Environ. Sci.: Atmos., 2025, **5**, 191–203 | **195**

variability in the field blank levels. Additionally, poorly sealed samplers, recording deployment time and date errors, and losses during analysis (such as catalyst failure) could have contributed to the observed results.

3.3 Hg concentrations and descriptive statistics

Table 1 lists the monthly average gaseous Hg concentrations obtained from the active *in situ* measurement and those derived from *Mer*PAS® using the OSR and AOSR, as well as the descriptive statistics. The mean of Hg concentrations derived with the AOSR (1.87 ng m^{-3}) and OSR (1.97 ng m^{-3}) was higher than the average Hg levels determined with the active *in situ* measurement (1.70 ng m^{-3}). These results are further explored through in-depth statistical analysis in subsequent sections.

3.4 Differences between active- and passive-derived gaseous Hg concentrations

The results of the Kruskal–Wallis test are presented in Fig. 2, showing the inferential statistics, estimate of effect size with its uncertainty, and pairwise comparisons. In addition, Fig. 2 visually represents the monthly average actively and passively derived gaseous Hg concentrations through a combination of violin, box, and jittered plots. These plots offer a comprehensive view of the data distribution. The box component of each plot presents descriptive statistics, including the 25th and 75th percentiles represented by the top and bottom lines, respectively. The middle line and red dot show the median and the boxplot whiskers indicate 95% of the data coverage; the axis is broken along the line to show outliers. Additionally, the violin plot, positioned on each side of the boxplot, provides additional information about the shape of the data distribution through
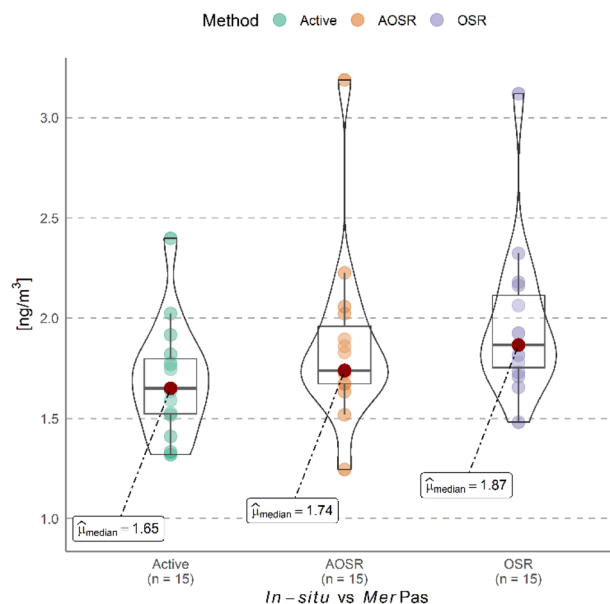

Fig. 2 A combination of a violin, box and jittered plot of the monthly average Hg concentrations determined with the active *in situ* sampler and *Mer*PAS® for different SRs. The top and bottom line shows the 25th and 75th percentile of concentration, and the middle line and red dot show the median. Whiskers on the boxplots show 95% coverage of the data; the axis is broken along the line to show outliers. The inferential statistics, an estimate of effect size and uncertainty, and pairwise comparisons are also shown.

kernel density estimation. The broader sections of the violin plot indicate a higher density of observations, while the skinnier sections represent a lower density.

The Kruskal–Wallis test indicated no statistically significant difference between Hg concentrations obtained from the active *in situ* and those derived from *Mer*PAS® OSR and AOSR (χ^2 (2, N = 45) = 5.50, p = 0.06). Although the p-value approached significance ($p < 0.05$), it remained slightly above this threshold, suggesting that observed variations likely reflect random differences rather than systematic ones between sampling methods. However, the effect size (ε^2 = 0.12) indicates that approximately 12% of the variability in Hg concentrations could be attributable to differences in sampling approach. While this effect is modest, the broad 95% confidence interval (0.02–1.00) reflects substantial uncertainty, highlighting the importance of further consideration of environmental and logistical factors impacting field measurements.

Further analysis using the Mann–Whitney U test reveals method-specific differences, with the OSR sampler showing a statistically significant 16% overestimation relative to active *in situ* measurement (W = 56.00, p = 0.020; r = −0.50, 95% CI [−0.75, −0.13]). In contrast, the AOSR showed a reduced, statistically nonsignificant overestimation of approximately 10% (W = 82.50, p = 0.221; r = −0.27, 95% CI [−0.60, 0.15]). The MND values are consistent with these findings, with the OSR yielding an MND of 17.42 ± 16.06%, while AOSR showed an improved MND of 12.65% ± 12.53%, suggesting that the AOSR

Table 1 Monthly averages and descriptive statistics of gaseous Hg concentrations (ng m^{-3}) determined with the active *in situ* measurement and derived from *Mer*PAS® using different SRs

Month	Active *in situ*	*Mer*PAS® OSR	*Mer*PAS® AOSR
06/2021	1.82	1.81	1.83
07/2021	2.40	3.12	3.19
08/2021	1.65	2.32	2.22
09/2021	1.32	1.93	1.74
10/2021	1.41	1.93	1.74
11/2021	1.59	2.16	1.89
12/2021	1.33	1.48	1.25
01/2022	1.75	1.78	1.63
02/2022	1.53	1.66	1.52
03/2022	1.92	2.18	2.06
04/2022	1.64	1.73	1.67
05/2022	2.02	2.06	2.02
06/2022	1.77	1.87	1.86
07/2022	1.77	1.71	1.67
08/2022	1.52	1.82	1.72
Mean	1.70	1.97	1.87
Median	1.65	1.87	1.74
SD	0.28	0.39	0.43
Min	1.32	1.48	1.25
Max	2.40	3.12	3.19

196 | *Environ. Sci.: Atmos.*, 2025, **5**, 191–203

© 2025 The Author(s). Published by the Royal Society of Chemistry

better approximates the active *in situ* data. Collectively, these results indicate that while *Mer*PAS® samplers provide estimates close to Tekran measurements, slight overestimations are present, particularly in challenging field conditions.

Environmental and logistical factors likely drive these differences. Deploying PAS at high-altitude sites such as Welgegund (1480 m asl) poses unique challenges due to lower atmospheric pressure. At higher elevations, reduced pressure enhances diffusion rates by increasing diffusion coefficients, yet it also decreases air density, resulting in less air mass per unit volume.[61,62] Although these effects theoretically counterbalance each other, the 16% overestimation of Hg concentrations at Welgegund points to a net increase in SR due to enhanced diffusion, aligning with similar findings from other high-altitude sites, such as Mt. Lulin and Mauna Loa. At these locations, passive samplers systematically overestimated Hg concentrations when compared to active *in situ* measurements (McLagan *et al.*[28]). Adjustments to the SR with wind speed and temperature appeared to mitigate these altitude-related influences, though variability persists.

Additional logistical constraints, such as this study's relative standard deviation (RSD%) for *Mer*PAS® samplers, was 14 ± 13%, higher than values reported in comparable studies. This elevated RSD% likely results from blank correction variability, deployment inconsistencies, and Hg content in blanks, which underscore the need for rigorous control in field protocols.

Another factor is the inherent uncertainty in active *in situ* measurements, estimated at 5–10%.[63,64] Although the active *in situ* in this study operated with a mass-flow controller to reduce pressure-induced variability, these intrinsic uncertainties likely propagated into comparisons. For example, the AOSR's 10% overestimation aligns with the upper range of active *in situ* uncertainty, suggesting that observed discrepancies reflect expected measurement variability rather than systematic bias.

Dynamic atmospheric conditions at Welgegund add another layer of variability. Shifts in air masses driven by natural and anthropogenic factors can lead to short-term fluctuations in Hg concentrations,[65,66] which may explain persistent overestimations in passive samplers despite AOSR adjustments. Comparable observations at the Maïdo Observatory (2160 m asl) showed that passive samplers overestimated Hg by 31% compared to Tekran, likely due to similar environmental dynamics.[46] While these results suggest that the *Mer*PAS® can provide comparable concentration estimates to the Tekran 2537X under the conditions of this study, a closer examination of several key factors is warranted to understand the implications of this comparison fully. Specifically, the challenges associated with sampling at high altitudes, the inherent uncertainties in active *in situ* measurements, and the potential propagation of these uncertainties into passive sampling calibration must be thoroughly addressed.

To further substantiate the earlier findings, Fig. 3 depicts the Spearman correlation of active *in situ* measurement against *Mer*PAS® OSR and AOSR in this study and PAS-derived Hg concentrations using McLagan *et al.*[28] recalibrated SR and adjusted SR. The figure also includes inferential statistics, such as effect size estimates, uncertainty, and pairwise comparisons.
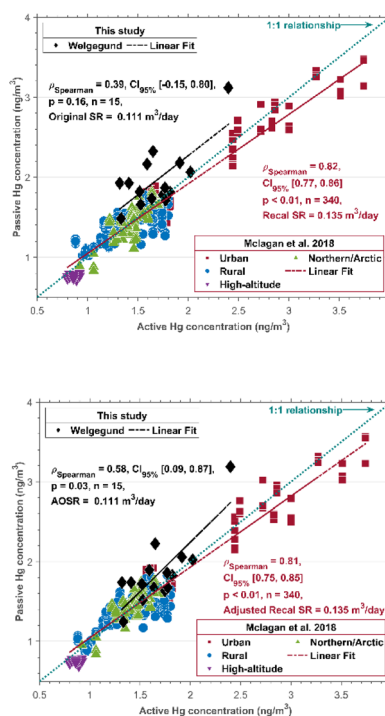

Fig. 3 Spearman correlation of active *in situ* measurement against *Mer*PAS® OSR and AOSR in this study and PAS-derived Hg concentrations using Mclagan *et al.* 2018 recalibrated SR and adjusted SR. The inferential statistics, an estimate of effect size and uncertainty, and pairwise comparisons are also shown. The dotted lines represent the trend line for each dataset. The dashed dark teal line is the 1:1 relationship.

The dotted lines represent trend lines for each dataset, while the dashed dark teal line indicates the 1:1 relationship. Markers are coloured based on site type: red for urban sites, blue for rural sites, purple for high-altitude sites, green for northern/Arctic sites, and black for Welgegund. The fitted relationship from McLagan *et al.*[28] combines all data and shows that the data points and the linear regression lines (dashed black for Welgegund and red for global sites) are positioned either above or below the 1:1 line, supporting the observation that *Mer*PAS® tends to overestimate Hg concentrations.

It is important to emphasize that the study by McLagan *et al.*[28] used the University of Toronto (UofT)-based mercury PAS, which differs from the commercialized *Mer*PAS®. Additionally, the UofT PAS and *Mer*PAS® operate with different sampling rates (SRs)-0.111 m³ per day for *Mer*PAS® *versus* 0.135 m³ per day for the UofT PAS. Consequently, any comparisons made between the UofT PAS data from McLagan *et al.*[28] and this study using *Mer*PAS® must be interpreted cautiously, as they are not directly comparable. Here, we use the PAS data to provide context and demonstrate where the results of this study align with the broader dataset.

Notably, even though Welgegund is a high-altitude site, its data are not closely aligned with the high-altitude sites from the McLagan *et al.*[28] study. This difference highlights the unique atmospheric conditions and pollution influences at Welgegund, which is situated in a region subject to frequent pollution

© 2025 The Author(s). Published by the Royal Society of Chemistry

Environ. Sci.: Atmos., 2025, **5**, 191–203 | 197

plumes from South Africa's industrial hubs. These factors likely play a significant role in the observed differences, and they underscore the distinct pollution regime at Welgegund compared to other high-altitude sites in McLagan et al.[28]

The correlation between passive and active gaseous Hg concentrations improves when adjusted sampling rates (SRs) are applied, as indicated by the reported Spearman correlation (ρ) values, which range from 0.39 to 0.58, representing moderate to significant positive correlations. However, the correlation between Active and OSR was not statistically significant ($p > 0.05$), while it was significant for concentrations derived from adjusted SRs ($p < 0.05$). These p-values suggest that the correlation between Active and OSR may be due to chance, but the correlations using adjusted SRs are more robust.

It is crucial to consider the wide confidence interval (95% CI) for both active and passive gaseous Hg concentrations across all graphs, ranging from -0.20 to 0.81. This indicates that the results are consistent with both negligible ($\rho = -0.20$) and significant ($\rho = 0.81$) relationships, making it challenging to draw definitive conclusions about the strength of the correlation.

Finally, the data from Welgegund cluster around the urban, rural, and northern/Arctic data points from McLagan et al.,[28] reinforcing that, while the site is classified as high-altitude, its regional atmospheric characteristics and proximity to significant anthropogenic pollution sources lead to a distinct pollution profile compared to McLagan's high-altitude sites. Welgegund frequently encounters pollution plumes from industrial hubs, including the Johannesburg-Pretoria megacity, the Vaal Triangle, the western Bushveld Complex, and the Mpumalanga Highveld. In addition, relatively clean air masses from the north-northwest to south-southwest sectors are also measured at the site, but their influence is less frequent compared to the dominant industrial emissions.

3.5 Bland–Altman analysis

In the sections above, statistical techniques like MND, Mann–Whitney U test, and Spearman correlation are commonly used to analyze the relationship between two variables. These techniques are helpful in identifying patterns, trends, or associations between the variables. However, they do not provide specific information about the level of agreement or disagreement between the two measurement methods. However, Bland–Altman analysis is a statistical method specifically designed to detect the presence of systematic differences between two measurement methods or instruments. It is particularly useful when comparing a new measurement method to an established or reference method. Like Silveira et al.[54] a three-step approach was applied to verify strict equivalence between the two measurement techniques. The first step involves evaluating the equivalence of structural means, which tests the similarity of accuracy between the two methods. The second step evaluates the equivalence of structural variances, determining whether the two measurement methods have similar variances when measuring the same samples. The third step involves testing the agreement with the structural bisector line, which tests for

equivalent measurements obtained from the same subject. This step determines whether a systematic difference exists between the two measurement methods for the same subject. Complete similarity can be established when all three tests showed non-rejection of equivalence at a 5% significance level.

3.5.1 Active *in situ* vs. *Mer*PAS® OSR and AOSR. The statistical analyses presented in Fig. 4 and 5 comprehensively evaluate the accuracy, precision, and reliability equivalence between active *in situ* and alternative Hg measurement approach – *Mer*PAS® OSR (Fig. 4) and *Mer*PAS® AOSR (Fig. 5).

Examining the accuracy plots (top panel), the (0,0) point representing perfect agreement falls outside the 95% confidence intervals for both *Mer*PAS® OSR and *Mer*PAS® AOSR. For *Mer*PAS® OSR, the 95% CI was [0.1079, 0.4257], while for *Mer*PAS® AOSR, it was [0.0241, 0.3202]. This indicates the *Mer*PAS® OSR and *Mer*PAS® AOSR exhibit statistically significant positive biases, overestimating the Hg concentrations compared to the active *in situ*.

The precision tests (middle panel) for both *Mer*PAS® OSR and *Mer*PAS® AOSR, the horizontal precision (x, 0) lines fell outside the 95% confidence bands, rejecting the null hypothesis of precision equivalence. This suggests the precision of the *Mer*PAS® derived concentration is not statistically comparable to active *in situ* measured concentration.

In contrast, the reliability tests (bottom panel) showed more promising results. For both *Mer*PAS® OSR and *Mer*PAS® AOSR, the bisector line representing perfect agreement was within the 95% confidence bands, supporting the reliability between these methods and active *in situ*.

Overall, the analyses presented in Fig. 4 and 5 provide a mixed picture regarding the equivalence of the active *in situ* compared to the *Mer*PAS® OSR and *Mer*PAS® AOSR. While the reliability tests suggest acceptable agreement, the accuracy and precision evaluations revealed statistically significant biases and a lack of precision equivalence. These findings indicate the *Mer*PAS® approach, when using OSR and AOSR to derive concentrations, may not be suitable replacement for the active *in situ* Hg measurement technique, at least based on the data shown. Further investigations would be needed to fully establish the comparability and interchangeability of these methods. Researchers and practitioners should consider the trade-offs carefully when selecting the appropriate Hg measurement approach for their applications.

3.6 Temporal pattern

In Fig. 6, the monthly Hg concentrations derived with the *Mer*PAS® using AOSR are presented together with the monthly average Hg levels determined by the active *in situ* measurements for the entire sampling period. Similar temporal patterns are observed for atmospheric Hg concentrations determined with AOSR and active *in situ* measurement. The seasonal average Hg levels determined with *Mer*PAS® using AOSR during winter 2021, spring 2021, summer 2021/2022, autumn 2022 and winter 2022 were 2.41, 1.79, 1.47, 1.92 and 1.75 ng m^{-3}, respectively. The seasonal mean Hg levels determined with the active *in situ* during winter 2021, spring 2021,
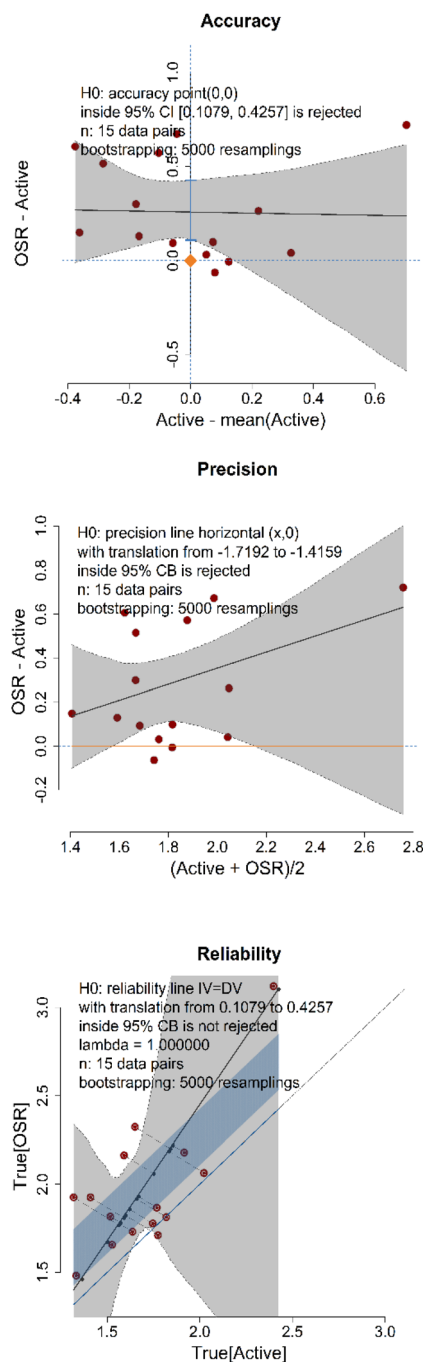
Fig. 4   Similarity of accuracy (top panel), precision (middle panel), and reliability (bottom panel) for active *in situ vs. Mer*PAS® OSR obtained with 5×10^3 bootstrap iterations.
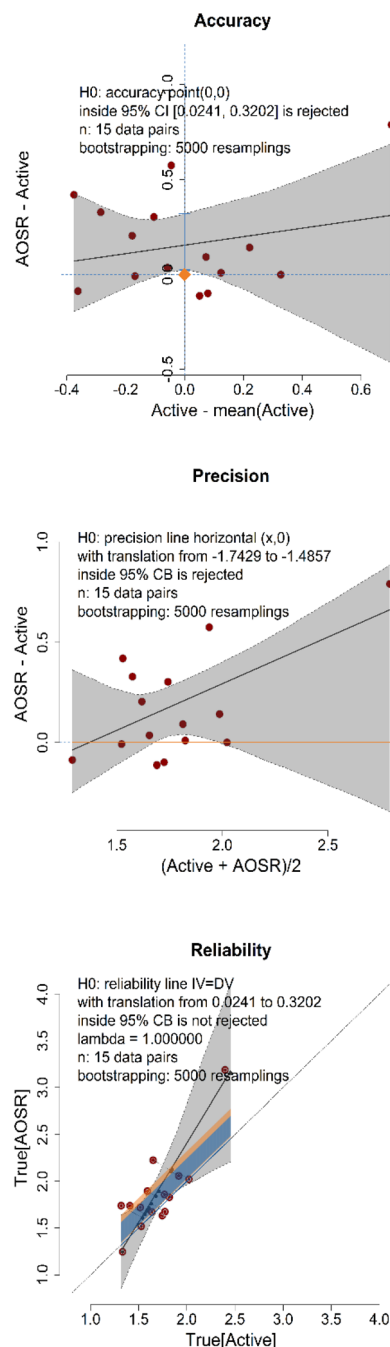

Fig. 5   Similarity of accuracy (top panel), precision (middle panel), and reliability (bottom panel) for active *in situ vs. Mer*PAS® AOSR obtained with 5×10^3 bootstrap iterations.

summer 2021/2022, autumn 2022 and winter 2022 were 1.96, 1.44, 1.54, 1.86 and 1.69 ng m^{-3}, respectively. No significant seasonal variation in Hg levels is evident during the 15 months sampling period, except for higher Hg concentrations determined during the winter of 2021. The highest monthly average Hg levels were determined in July 2021 with *Mer*PAS® and the active *in situ* measurement. Increases in concentrations of atmospheric pollutants typically occur in South Africa due to more pronounced low-level inversion layers trapping

pollutants near the surface and changes in pollutant sources contribution, such as increased household combustion for space heating (*e.g.* Laban *et al.*, 2018; Lourens *et al.*, 2011)[33,67]. However, increased atmospheric Hg concentrations are not observed during the winter of 2022, with Hg levels being similar to other seasons. This difference between Hg concentrations determined during the winter seasons in 2021 and 2022 could be attributed to changes in air mass movement passing over source regions impacting Welgegund, which could be assessed through in-depth air mass back trajectory
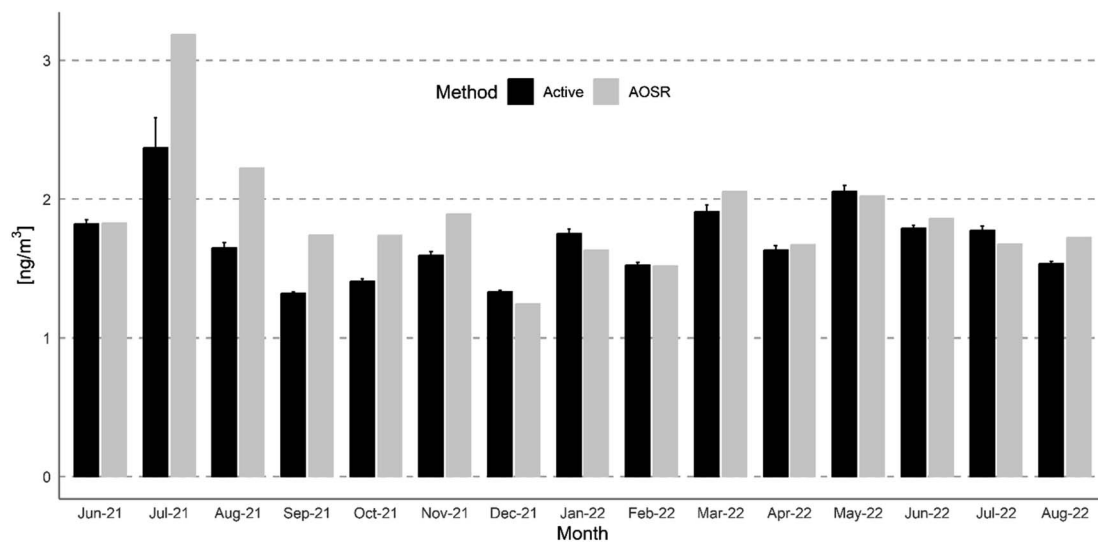
Fig. 6 Comparison of the monthly average Hg concentrations determined with *Mer*PAS® AOSR (grey) and active *in situ* (black) during the sampling period.

analysis. However, this type of analysis was beyond the scope of this study and will be conducted in future research where longer-term (at least two full years) active *in situ* atmospheric Hg measurements conducted at Welgegund will be explored. The lowest seasonal average Hg concentrations were determined in summer with *Mer*PAS® and in spring with the active *in situ* measurement.

4 Conclusions

This study compared atmospheric Hg concentrations using a passive sampling method, *Mer*PAS®, and active *in situ* measurements at a regional background site in South Africa between June 2021 and September 2022. *Mer*PAS® was evaluated using two sampling rates: the original sampling rate (OSR) and the adjusted original sampling rate (AOSR). This comparison offers valuable insights into the effectiveness and reliability of these sampling techniques for accurate atmospheric Hg monitoring.

Various statistical tests were conducted to analyze differences between the passive and active sampling techniques, including the Kruskal–Wallis test, Mann–Whitney U test, Spearman correlation, and Bland–Altman analysis. Results indicated that Hg concentrations obtained using *Mer*PAS® with the OSR and AOSR generally showed higher values compared to active *in situ* measurements. However, using the AOSR helped reduce some of the uncertainty associated with *Mer*PAS® measurements, as reflected in the Mean Normalized Difference (MND) values. The findings in this study indicate a need for adjusted sampling rates like the AOSR to improve *Mer*PAS®'s accuracy when compared to active *in situ* measurements.

Further statistical analyses revealed no statistically significant differences in Hg concentrations obtained from the two sampling techniques. The Mann–Whitney U test clarified the extent of overestimating Hg levels, while the Spearman correlation supported observations that *Mer*PAS® tends to

overestimate Hg levels. The Bland–Altman analysis confirmed reliability, while the accuracy and precision evaluations were not statistically comparable to active *in situ* measurements.

While this statistical analysis revealed improved accuracy with AOSR, it did not consider the impact of various atmospheric factors, such as Hg emissions sources, deposition processes, long-range transport, and chemical transformations, on Hg levels measured by *Mer*PAS®. The dataset used was relatively small, which posed specific challenges in the statistical analysis of Hg concentrations. These challenges included: (1) limited statistical power, making it difficult to detect minor yet potentially meaningful differences in Hg levels; (2) higher uncertainty in statistical estimates, affecting the precision and reliability of conclusions; (3) reduced generalizability of findings, limiting the study's representation of Hg variability across different environmental conditions and timeframes; and (4) increased sensitivity of results to small changes in the dataset or analysis approach, which may reduce reproducibility.

Based on our findings, we recommend using AOSR for Hg monitoring at sites in southern Africa where *Mer*PAS® is deployed. Nonetheless, it is important to acknowledge these limitations and the need for further research. Larger datasets and a more in-depth investigation of Hg concentrations' mechanisms would improve our understanding of seasonal patterns and factors affecting passive sampling measurements.

In conclusion, this study contributes valuable insights into atmospheric Hg monitoring by statistically evaluating passive and active sampling techniques. Future studies, ideally with larger datasets and a stronger focus on underlying environmental mechanisms, can refine our understanding and enhance the accuracy of Hg monitoring in diverse field conditions.

Data availability

The data supporting the findings of this study are available and have been included in the ESI.†

200 | *Environ. Sci.: Atmos.*, 2025, **5**, 191–203

© 2025 The Author(s). Published by the Royal Society of Chemistry

Author contributions

Conflicts of interest

There are no conflicts of interest to declare.

Acknowledgements

References

1 N. Pirrone, S. Cinnirella, X. Feng, R. B. Finkelman, H. R. Friedli, J. Leaner, R. Mason, A. B. Mukherjee, G. B. Stracher, D. G. Streets and K. Telmer, Global mercury emissions to the atmosphere from anthropogenic and natural sources, *Atmos. Chem. Phys.*, 2010, **10**, 5951–5964.

2 K. E. Masekoameng, J. Leaner and J. Dabrowski, Trends in anthropogenic mercury emissions estimated for South Africa during 2000–2006, *Atmos. Environ.*, 2010, **44**, 3007–3014.

3 S. Zhao, D. Pudasainee, Y. Duan, R. Gupta, M. Liu and J. Lu, A review on mercury in coal combustion process: Content and occurrence forms in coal, transformation, sampling methods, emission and control technologies, *Prog. Energy Combust. Sci.*, 2019, **73**, 26–64.

4 G. M. Scott and T. N. Mdluli, The Minamata Treaty/Protocol: Potential Implications for South Africa, *Clean Air J.*, 2012, **22**, 17–19.

5 J. A. Fisher, L. Schneider, A.-H. Fostier, S. Guerrero, J. R. D. Guimarães, C. Labuschagne, J. J. Leaner, L. G. Martin, R. P. Mason and V. Somerset, A synthesis of mercury research in the Southern Hemisphere, part 2: Anthropogenic perturbations, *Ambio*, 2023, **52**, 918–937.

6 W. H. Schroeder and J. Munthe, Atmospheric mercury - An overview, *Atmos. Environ.*, 1998, **32**, 809–822.

7 N. E. Selin, Global Biogeochemical Cycling of Mercury: A Review, *Annual Review of Environment and Resources*, 2009, **34**, 43–63.

8 C. T. Driscoll, R. P. Mason, H. M. Chan, D. J. Jacob and N. Pirrone, Mercury as a global pollutant: Sources, pathways, and effects, *Environ. Sci. Technol.*, 2013, **47**, 4967–4983.

9 J. Li and S. Lee, Progress of global atmospheric mercury field observations, J, *J. Clean Energy Technol.*, 2014, **2**, 252–257.

10 C. J. Lin, P. Pongprueksa, S. E. Lindberg, S. O. Pehkonen, D. Byun and C. Jang, Scientific uncertainties in atmospheric mercury models I: Model science evaluation, *Atmos. Environ.*, 2006, **40**, 2911–2928.

11 O. Travnikov, H. Angot, P. Artaxo, M. Bencardino, J. Bieser, F. D'Amore, A. Dastoor, F. De Simone, M. D. C. Diéguez, A. Dommergue, R. Ebinghaus, X. B. Feng, C. N. Gencarelli, I. M. Hedgecock, O. Magand, L. Martin, V. Matthias, N. Mashyanov, N. Pirrone, R. Ramachandran, K. A. Read, A. Ryjkov, N. E. Selin, F. Sena, S. Song, F. Sprovieri, D. Wip, I. Wängberg and X. Yang, Multi-model study of mercury dispersion in the atmosphere: atmospheric processes and model evaluation, *Atmos. Chem. Phys.*, 2017, **17**, 5271–5295.

12 N. Pirrone, W. Aas, S. Cinnirella, R. Ebinghaus, I. M. Hedgecock, J. Pacyna, F. Sprovieri and E. M. Sunderland, Toward the next generation of air quality monitoring: Mercury, *Atmos. Environ.*, 2013, **80**, 599–611.

13 F. Sprovieri, N. Pirrone, M. Bencardino, F. D'Amore, H. Angot, C. Barbante, E. G. Brunke, F. Arcega-Cabrera, W. Cairns, S. Comero, M. Del Carmen Diéguez, A. Dommergue, R. Ebinghaus, X. Bin Feng, X. Fu, P. Elizabeth Garcia, B. Manfred Gawlik, U. Hageström, K. Hansson, M. Horvat, J. Kotnik, C. Labuschagne, O. Magand, L. Martin, N. Mashyanov, T. Mkololo, J. Munthe, V. Obolkin, M. Ramirez Islas, F. Sena, V. Somerset, P. Spandow, M. Vardè, C. Walters, I. Wängberg, A. Weigelt, X. Yang and H. Zhang, Five-year records of mercury wet deposition flux at GMOS sites in the Northern and Southern hemispheres, *Atmos. Chem. Phys.*, 2017, **17**, 2689–2708.

14 P. Baker, E.-G. Brunke, F. Slemr and A. Crouch, Atmospheric mercury measurements at cape point, south africa, *Atmos. Environ.*, 2002, **36**, 2459–2465.

15 F. Slemr, E. G. Brunke, C. Labuschagne and R. Ebinghaus, Total gaseous mercury concentrations at the Cape Point GAW station and their seasonality, *Geophys. Res. Lett.*, 2008, **35**, DOI: 10.1029/2008GL033741.

16 L. G. Martin, C. Labuschagne, E.-G. Brunke, A. Weigelt, R. Ebinghaus and F. Slemr, Trend of atmospheric mercury concentrations at Cape Point for 1995–2004 and since 2007, *Atmos. Chem. Phys.*, 2017, **17**, 2393–2399.

17 A. Venter, J. Beukes, P. Van Zyl, E.-G. Brunke, C. Labuschagne, F. Slemr, R. Ebinghaus and H. Kock, Statistical exploration of gaseous elemental mercury (GEM) measured at Cape Point from 2007 to 2011, *Atmos. Chem. Phys.*, 2015, **15**, 10271–10280.

© 2025 The Author(s). Published by the Royal Society of Chemistry

Environ. Sci.: Atmos., 2025, **5**, 191–203 | **201**

18 E. G. Brunke, C. Labuschagne and F. Slemr, Gaseous mercury emissions from a fire in the Cape Peninsula, South Africa, during January 2000, *Geophys. Res. Lett.*, 2001, **28**, 1483–1486.

19 J. J. Leaner, J. M. Dabrowski, R. P. Mason, T. Resane, M. Richardson, M. Ginster, G. Gericke, C. R. Petersen, E. Masekoameng and P. J. Ashton, in *Mercury Fate and Transport in the Global Atmosphere: Emissions, Measurements and Models*, Springer, 2009, pp. 113–130.

20 J. Bieser, H. Angot, F. Slemr and L. Martin, Atmospheric mercury in the southern hemisphere–Part 2: source apportionment analysis at Cape point station, South Africa, *Atmos. Chem. Phys.*, 2020, **20**, 10427–10439.

21 M. D. Belelie, S. J. Piketh, R. P. Burger, A. D. Venter and M. Naidoo, Characterisation of ambient Total Gaseous Mercury concentrations over the South African Highveld, *Atmos. Pollut. Res.*, 2019, **10**, 12–23.

22 R. Meyer, North-West University, South Africa, 2019.

23 D. S. McLagan, C. P. J. Mitchell, H. Huang, Y. D. Lei, A. S. Cole, A. Steffen, H. Hung and F. Wania, A High-Precision Passive Air Sampler for Gaseous Mercury, *Environ. Sci. Technol. Lett.*, 2016, **3**, 24–29.

24 J. Huang, S. N. Lyman, J. S. Hartman and M. S. Gustin, A review of passive sampling systems for ambient air mercury measurements, *Environ. Sci.: Processes Impacts*, 2014, **16**, 374–392.

25 F. Wania and C. Shunthirasingham, Passive air sampling for semi-volatile organic chemicals, *Environ. Sci.: Processes Impacts*, 2020, **22**, 1925–2002.

26 A. Naccarato, A. Tassone, M. Martino, S. Moretti, A. Macagnano, E. Zampetti, P. Papa, J. Avossa, N. Pirrone, M. Nerentorp, J. Munthe, I. Wängberg, G. W. Stupple, C. P. J. Mitchell, A. R. Martin, A. Steffen, D. Babi, E. M. Prestbo, F. Sprovieri and F. Wania, A field intercomparison of three passive air samplers for gaseous mercury in ambient air, *Atmos. Meas. Tech.*, 2021, **14**, 3657–3672.

27 D. S. McLagan, B. A. Hussain, H. Huang, Y. D. Lei, F. Wania and C. P. J. Mitchell, Identifying and evaluating urban mercury emission sources through passive sampler-based mapping of atmospheric concentrations, *Environ. Res. Lett.*, 2018, **13**, 074008.

28 D. S. McLagan, C. P. J. Mitchell, A. Steffen, H. Hung, C. Shin, G. W. Stupple, M. L. Olson, W. T. Luke, P. Kelley, D. Howard, G. C. Edwards, P. F. Nelson, H. Xiao, G. R. Sheu, A. Dreyer, H. Huang, B. Abdul Hussain, Y. D. Lei, I. Tavshunsky and F. Wania, Global evaluation and calibration of a passive air sampler for gaseous mercury, *Atmos. Chem. Phys.*, 2018, **18**, 5905–5919.

29 W. Booyens, P. G. Van Zyl, J. P. Beukes, J. Ruiz-Jimenez, M. Kopperi, M.-L. Riekkola, M. Josipovic, A. D. Venter, K. Jaars, L. Laakso, V. Vakkari, M. Kulmala and J. J. Pienaar, Size-resolved characterisation of organic compounds in atmospheric aerosols collected at Welgegund, South Africa, *J. Atmos. Chem.*, 2015, **72**, 43–64.

30 K. Jaars, J. P. Beukes, P. G. van Zyl, A. D. Venter, M. Josipovic, J. J. Pienaar, V. Vakkari, H. Aaltonen, H. Laakso, M. Kulmala, P. Tiitta, A. Guenther, H. Hellen, L. Laakso and H. Hakola, Ambient aromatic hydrocarbon measurements at Welgegund, South Africa, *Atmos. Chem. Phys.*, 2014, **14**, 7075–7089.

31 K. Jaars, P. G. van Zyl, J. P. Beukes, H. Hellen, V. Vakkari, M. Josipovic, A. D. Venter, M. Rasanen, L. Knoetze, D. P. Cilliers, S. J. Siebert, M. Kulmala, J. Rinne, A. Guenther, L. Laakso and H. Hakola, Measurements of biogenic volatile organic compounds at a grazed savannah grassland agricultural landscape in South Africa, *Atmos. Chem. Phys.*, 2016, **16**, 15665–15688.

32 K. Jaars, M. Vestenius, P. G. van Zyl, J. P. Beukes, H. Hellen, V. Vakkari, M. Venter, M. Josipovic and H. Hakola, Receptor modelling and risk assessment of volatile organic compounds measured at a regional background site in South Africa, *Atmos. Environ.*, 2018, **172**, 133–148.

33 T. L. Laban, P. G. Van Zyl, J. Paul Beukes, V. Vakkari, K. Jaars, N. Borduas-Dedekind, M. Josipovic, A. Mee Thompson, M. Kulmala and L. Laakso, Seasonal influences on surface ozone variability in continental South Africa and implications for air quality, *Atmos. Chem. Phys.*, 2018, **18**, 15491–15514.

34 A. D. Venter, P. G. van Zyl, J. P. Beukes, M. Josipovic, J. Hendriks, V. Vakkari and L. Laakso, Atmospheric trace metals measured at a regional background site (Welgegund) in South Africa, *Atmos. Chem. Phys.*, 2017, **17**, 4251–4263.

35 A. D. Venter, P. G. van Zyl, J. P. Beukes, J.-S. Swartz, M. Josipovic, V. Vakkari, L. Laakso and M. Kulmala, Size-resolved characteristics of inorganic ionic species in atmospheric aerosols at a regional background site on the South African Highveld, *J. Atmos. Chem.*, 2018, **75**, 285–304.

36 M. Venter, J. P. Beukes, P. G. van Zyl, V. Vakkari, A. Virkkula, M. Josipovic, M. Kulmala and L. Laakso, Six-year observations of aerosol optical properties at a southern African grassland savannah site, *Atmos. Environ.*, 2020, **230**, 117477.

37 D. S. McLagan, M. E. E. Mazur, C. P. J. Mitchell and F. Wania, Passive air sampling of gaseous elemental mercury: a critical review, *Atmos. Chem. Phys.*, 2016, **16**, 3061–3076.

38 D. S. McLagan, C. P. Mitchell, H. Huang, B. Abdul Hussain, Y. D. Lei and F. Wania, The effects of meteorological parameters and diffusive barrier reuse on the sampling rate of a passive air sampler for gaseous mercury, *Atmos. Meas. Tech.*, 2017, **10**, 3651–3660.

39 D. S. McLagan, F. Monaci, H. Y. Huang, Y. D. Lei, C. P. J. Mitchell and F. Wania, Characterization and Quantification of Atmospheric Mercury Sources Using Passive Air Samplers, *J. Geophys. Res.:Atmos.*, 2019, **124**, 2351–2362.

40 D. S. McLagan, S. Osterwalder and H. Biester, Temporal and spatial assessment of gaseous elemental mercury concentrations and emissions at contaminated sites using active and passive measurements, *Environ. Res. Commun.*, 2021, **3**, 051004.

41 M. A. Lopez-Anton, Y. Yuan, R. Perry and M. M. Maroto-Valer, Analysis of mercury species present during coal combustion by thermal desorption, *Fuel*, 2010, **89**, 629–634.

42 J. V. Cizdziel, T. A. Hinners and E. M. Heithmar, Determination of total mercury in fish tissues using combustion atomic absorption spectrometry with gold amalgamation, *Water, Air, Soil Pollut.*, 2002, **135**, 355–370.

43 J. Chen, P. Chakravarty, G. R. Davidson, D. G. Wren, M. A. Locke, Y. Zhou, G. Brown Jr and J. V. Cizdziel, Simultaneous determination of mercury and organic carbon in sediment and soils using a direct mercury analyzer based on thermal decomposition-atomic absorption spectrophotometry, *Anal. Chim. Acta*, 2015, **871**, 9–17.

44 D. S. McLagan, H. Huang, Y. D. Lei, F. Wania and C. P. Mitchell, Application of sodium carbonate prevents sulphur poisoning of catalysts in automated total mercury analysis, *Spectrochim. Acta, Part B*, 2017, **133**, 60–62.

45 D. S. McLagan, C. P. J. Mitchell, H. Huang, Y. D. Lei, A. S. Cole, A. Steffen, H. Hung and F. Wania, A High-Precision Passive Air Sampler for Gaseous Mercury, *Environ. Sci. Technol. Lett.*, 2016, **3**, 24–29.

46 C. Hoang, O. Magand, J. Brioude, A. Dimuro, C. Brunet, C. Ah-Peng, Y. Bertrand, A. Dommergue, Y. D. Lei and F. Wania, Probing the limits of sampling gaseous elemental mercury passively in the remote atmosphere, *Environ. Sci.: Atmos.*, 2023, **3**, 268–281.

47 R. C. Team, *R: A language and environment for statistical computing, R Foundation for Statistical Computing*, 2013.

48 H. Wickham, W. Chang and M. H. Wickham, *Package 'ggplot2', Create elegant data visualisations using the grammar of graphics*, 2016, vol. 2, pp. 1-189.

49 H. Wickham, M. Averick, J. Bryan, W. Chang, L. D. A. McGowan, R. François, G. Grolemund, A. Hayes, L. Henry and J. Hester, Welcome to the Tidyverse, *Journal of open source software*, 2019, **4**, 1686.

50 A. Kassambara, *rstatix: pipe-friendly framework for basic statistical tests*, 2023, DOI: **10.32614/CRAN.package.rstatix**.

51 P. Aphalo, K. Slowikowski and S. Mouksassi, *Package 'ggpmisc': miscellaneous extensions to 'ggplot2', R package, version 0.5.0*, 2022, DOI: **10.32614/CRAN.package.ggpmisc**.

52 I. Patil, Visualizations with statistical details: The 'ggstatsplot' approach, *The Journal of Open Source Software*, 2021, **6**, 3167.

53 J. Cohen, Statistical power analysis, *Current directions in psychological science*, 1992, **1**, 98–101.

54 P. S. P. Silveira, J. E. Vieira and J. d. O. Siqueira, Is the Bland-Altman plot method useful without inferences for accuracy, precision, and agreement?, *Rev. Saude Publica*, 2024, **58**, 01.

55 M. I. Quant, M. Feigis, S. Mistry, Y. D. Lei, C. P. J. Mitchell, R. Staebler, A. Di Guardo, E. Terzaghi and F. Wania, Using Passive Air Samplers to Quantify Vertical Gaseous Elemental Mercury Concentration Gradients Within a Forest and Above Soil, *J. Geophys. Res.:Atmos.*, 2021, **126**, e2021JD034981.

56 M. A. Snow, G. Darko, O. Gyamfi, E. Ansah, K. Breivik, C. Hoang, Y. D. Lei and F. Wania, Characterization of inhalation exposure to gaseous elemental mercury during artisanal gold mining and e-waste recycling through combined stationary and personal passive sampling, *Environ. Sci.:Processes Impacts*, 2021, **23**, 569–579.

57 M. Si, D. S. McLagan, A. Mazot, N. Szponar, B. Bergquist, Y. D. Lei, C. P. J. Mitchell and F. Wania, Measurement of Atmospheric Mercury over Volcanic and Fumarolic Regions on the North Island of New Zealand Using Passive Air Samplers, *ACS Earth Space Chem.*, 2020, **4**, 2435–2443.

58 H. Skov, B. T. Sørensen, M. S. Landis, M. S. Johnson, P. Sacco, M. E. Goodsite, C. Lohse and K. S. Christiansen, Performance of a new diffusive sampler for Hg0 determination in the troposphere, *Environ. Chem.*, 2007, **4**, 75–80.

59 W. Zhang, Y. Tong, D. Hu, L. Ou and X. Wang, Characterization of atmospheric mercury concentrations along an urban–rural gradient using a newly developed passive sampler, *Atmos. Environ.*, 2012, **47**, 26.

60 I.-G. Cho, D.-W. Hwang, S. Y. Kwon and S.-D. Choi, Optimization and application of passive air sampling method for gaseous elemental mercury in Ulsan, South Korea, *Environ. Sci. Pollut. Res.*, 2023, **30**, 17257–17267.

61 J. M. Armitage, S. J. Hayward and F. Wania, Modeling the uptake of neutral organic chemicals on XAD passive air samplers under variable temperatures, external wind speeds and ambient air concentrations (PAS-SIM), *Environ. Sci. Technol.*, 2013, **47**, 13546–13554.

62 J. Klánová, P. Èupr, J. i. Kohoutek and T. Harner, Assessing the influence of meteorological parameters on the performance of polyurethane foam-based passive air samplers, *Environ. Sci. Technol.*, 2008, **42**, 550–555.

63 K. Aspmo, P.-A. Gauchard, A. Steffen, C. Temme, T. Berg, E. Bahlmann, C. Banic, A. Dommergue, R. Ebinghaus and C. Ferrari, Measurements of atmospheric mercury species during an international study of mercury depletion events at Ny-Ålesund, Svalbard, spring 2003. How reproducible are our present methods?, *Atmos. Environ.*, 2005, **39**, 7607–7619.

64 C. Temme, P. Blanchard, A. Steffen, C. Banic, S. Beauchamp, L. Poissant, R. Tordon and B. Wiens, Trend, seasonal and multivariate analysis study of total gaseous mercury data from the Canadian atmospheric mercury measurement network (CAMNet), *Atmos. Environ.*, 2007, **41**, 5423.

65 J. Bieser, F. Slemr, J. Ambrose, C. Brenninkmeijer, S. Brooks, A. Dastoor, F. DeSimone, R. Ebinghaus, C. N. Gencarelli and B. Geyer, Multi-model study of mercury dispersion in the atmosphere: vertical and interhemispheric distribution of mercury species, *Atmos. Chem. Phys.*, 2017, **17**, 6925–6955.

66 F. Carbone, A. Bruno, A. Naccarato, F. De Simone, C. N. Gencarelli, F. Sprovieri, I. M. Hedgecock, M. Landis, H. Skov and K. A. Pfaffhuber, The superstatistical nature and interoccurrence time of atmospheric mercury concentration fluctuations, *J. Geophys. Res.:Atmos.*, 2018, **123**, 764–774.

67 A. S. Lourens, G. D. Fourie, J. W. Burger, J. J. Pienaar, C. E. Read, J. H. Jordaan, P. G. Van Zyl and J. P. Beukes, Spatial and temporal assessment of gaseous pollutants in the Highveld of South Africa, *S. Afr. J. Sci.*, 2011, **107**, 1–8.

© 2025 The Author(s). Published by the Royal Society of Chemistry

Environ. Sci.: Atmos., 2025, **5**, 191–203 | **203**